

THE COSMIC DECLINE IN THE H₂/HI-RATIO IN GALAXIES

D. OBRESCHKOW AND S. RAWLINGS

Astrophysics, Department of Physics, University of Oxford, Keble Road, Oxford, OX1 3RH, UK

ApJL, Accepted 2009 April 14

ABSTRACT

We use a pressure-based model for splitting cold hydrogen into its atomic (HI) and molecular (H₂) components to tackle the co-evolution of HI, H₂, and star formation rates (SFR) in $\sim 3 \cdot 10^7$ simulated galaxies in the Millennium Simulation. The main prediction is that galaxies contained similar amounts of HI at redshift $z \approx 1 - 5$ than today, but substantially more H₂, in quantitative agreement with the strong molecular line emission already detected in a few high-redshift galaxies and approximately consistent with inferences from studies of the damped Lyman- α absorbers seen in the spectra of quasars. The cosmic H₂/HI-ratio is predicted to evolve monotonically as $\Omega_{\text{H}_2}/\Omega_{\text{HI}} \propto (1+z)^{1.6}$. This decline of the H₂/HI-ratio as a function of cosmic time is driven by the growth of galactic disks and the progressive reduction of the mean cold gas pressure. Finally, a comparison between the evolutions of HI, H₂, and SFRs reveals two distinct cosmic epochs of star formation: an early epoch ($z \gtrsim 3$), driven by the evolution of $\Omega_{\text{HI}+\text{H}_2}(z)$, and a late epoch ($z \lesssim 3$), driven by the evolution of $\Omega_{\text{H}_2}(z)/\Omega_{\text{HI}}(z)$.

Subject headings: galaxies: high-redshift — galaxies: evolution — ISM: atoms — ISM: molecules — cosmology: theory

1. INTRODUCTION AND KEY IDEA

Neutral hydrogen is the fuel for the formation of stars. The cosmic star formation rate (SFR) density as inferred from ultraviolet, far-infrared, and submillimeter observations increases by an order of magnitude from redshift $z = 0$ to $z = 2$ (Hopkins 2007). Hence, neutral hydrogen in early galaxies was either more abundant or transformed into stars more efficiently than today.

A useful quantity in this context is the star formation efficiency (SFE) of a galaxy, defined as the SFR divided by the gas mass. The weak cosmic evolution of the density of neutral atomic hydrogen (HI), derived from Lyman-alpha absorption against distant quasars (Lah et al. 2007; Pontzen & Pettini 2009), indicates a strongly increased SFE at high z . But recent detections of strong molecular line emission in ordinary galaxies at $z = 1.5$ (Daddi et al. 2008) suggest that the SFEs of these galaxies are similar to those seen today. The seeming contradiction between these two conclusions arises from the conceptual confusion of SFEs inferred from galactic HI with those inferred from H₂. In fact, it is crucial to distinguish between the two quantities $\text{SFE}_{\text{HI}} \equiv \text{SFR}/M_{\text{HI}}$ and $\text{SFE}_{\text{H}_2} \equiv \text{SFR}/M_{\text{H}_2}$. In principle, there is no contradiction between the detected strong cosmic evolution of SFE_{HI} and the weak evolution of SFE_{H_2} – these empirical findings could simply imply that the H₂/HI-mass ratios $R_{\text{mol}}^{\text{galaxy}}$ of galaxies increase substantially with z .

In this letter, we show that there is indeed strong theoretical support for such an increase of $R_{\text{mol}}^{\text{galaxy}}$ with z in regular galaxies. This evolution is driven by the approximate scaling of galaxy sizes as $(1+z)^{-1}$ predicted by dark matter theory (Gunn & Gott 1972) and confirmed by observations in the Ultra Deep Field (Bouwens et al. 2004). Hence, the cold gas disks at high redshift must, on average, be denser than today. Combining this prediction with the relation between gas pressure and H₂/HI-ratios in nearby galaxies (e.g. Blitz & Rosolowsky 2006), leads to the conclusion that $R_{\text{mol}}^{\text{galaxy}}$ must increase dramatically with z . Our quantita-

tive predictions of this evolution rely on a recently presented semi-analytic numerical simulation of HI and H₂ in $\sim 3 \cdot 10^7$ simulated galaxies (Obreschkow et al. 2009), based on the Millennium Simulation (Springel et al. 2005).

Section 2 overviews our simulation method and the model for the H₂/HI-ratio in galaxies. In Section 3, we present and interpret the predicted evolution of galactic HI and H₂ and their relation to star formation. Section 4 compares these predictions to empirical data, and Section 5 summarizes our key conclusions.

2. SIMULATING HI AND H₂ IN GALAXIES

2.1. Physical model for galactic H₂/HI-ratios

In virtually all regular galaxies in the local Universe, whether spirals (e.g. Leroy et al. 2008) or ellipticals (e.g. Young 2002), the cold gas resides in a flat disk. Some observations of CO at $z \approx 2$ (Tacconi et al. 2006) suggest that even at high redshift most cold gas lies in disks. Based on this evidence, we have recently introduced a model for the distributions of HI and H₂ in regular galaxies (Obreschkow et al. 2009), assuming that all cold gas resides in a flat symmetric disk with an exponential surface density profile and that the local H₂/HI-ratio is dictated by the kinematic gas pressure (Blitz & Rosolowsky 2006; Leroy et al. 2008). Within these assumptions, we could show that the H₂/HI-mass ratio $R_{\text{mol}}^{\text{galaxy}}$ of an entire galaxy is given by

$$R_{\text{mol}}^{\text{galaxy}} = (3.44 R_{\text{mol}}^{\text{c}})^{-0.506} + 4.82 R_{\text{mol}}^{\text{c} - 1.054})^{-1}, \quad (1)$$

where $R_{\text{mol}}^{\text{c}}$ represents the H₂/HI-ratio at the galaxy center. $R_{\text{mol}}^{\text{c}}$ can be approximated as

$$R_{\text{mol}}^{\text{c}} = [11.3 \text{ m}^4 \text{ kg}^{-2} r_{\text{disk}}^{-4} M_{\text{g}} (M_{\text{g}} + 0.4 M_{\text{s}}^{\text{disk}})]^{0.8}, \quad (2)$$

where r_{disk} is the exponential scale radius of the disk, M_{g} is the total cold gas mass, and $M_{\text{s}}^{\text{disk}}$ is the stellar mass in the disk. Eqs. (1,2) constitute a physical model to estimate $R_{\text{mol}}^{\text{galaxy}}$ in regular galaxies based on $M_{\text{s}}^{\text{disk}}$, M_{g} , and

r_{disk} . In order to predict the cosmic evolution of $R_{\text{mol}}^{\text{galaxy}}$, we therefore require a model for the co-evolution of $M_{\text{s}}^{\text{disk}}$, M_{g} , and r_{disk} in galaxies. To this end, we adopted the virtual galaxy catalog of the Millennium Simulation described in Section 2.2. The limitations of the model of eqs. (1,2) and their impact on the predicted H_2/HI -ratios are discussed in (Obreschkow et al. 2009).

2.2. HI and H₂ in the Millennium Simulation

The Millennium Simulation (Springel et al. 2005) is an N -body simulation within the Λ CDM cosmology of $\sim 10^{10}$ gravitationally interacting particles in a periodic box of comoving volume $(500 h^{-1} \text{ Mpc})^3$, where $H_0 = 100 h \text{ km s}^{-1} \text{ Mpc}^{-1}$ and $h = 0.73$. The evolving large-scale structure generated by this simulation served as the skeleton for the simulation of $\sim 3 \cdot 10^7$ galaxies at the halo centers. In the “semi-analytic” approach adopted by De Lucia & Blaizot (2007), galaxies were considered as simplistic objects with a few global properties that are evolved stepwisely using a list of physical prescriptions. For example, the total amount of cold hydrogen ($\text{HI} + \text{H}_2$) in a galaxy is defined by the history of the net accretion, which in the model consists of (i) the infall of gas from the hot halo, (ii) the loss of gas by star formation, and (iii) outflows driven by supernovae and active galactic nuclei. Star formation in each galaxy is tackled using a law, where all cold gas above a critical surface density is transformed into stars on a timescale proportional to the dynamical time of the disk (for details see Croton et al. 2006).

In Obreschkow et al. (2009), we applied the model of Section 2.1 to the simulated galaxies in the catalog of De Lucia & Blaizot (2007) (“DeLucia-catalog”), to split their cold hydrogen masses into HI and H_2 . Our simulation successfully reproduced many local observations of HI and H_2 , such as mass functions (MFs), mass–diameter relations, and mass–velocity relations. Yet, the high-redshift predictions are inevitably limited by the semi-analytic recipes of the DeLucia-catalog. The most uncertain recipes are those related to mergers (e.g. feedback of black hole coalescence and starbursts), but they have a minor effect on the cosmic space densities of HI and H_2 , since most cold gas in the simulation is found in regular disk galaxies¹ with at most minor merger histories. However, inaccurate prescriptions for isolated galaxies could significantly affect the space densities of HI and H_2 , and it may well become necessary to refine our simulation as improved semi-analytic methods come on line.

3. RESULTS

3.1. Predicted evolution of HI and H₂

Fig. 1 shows the predicted evolution of the HI -MF and H_2 -MF, i.e. the comoving space densities of sources per logarithmic mass interval. The predictions at $z = 0$ roughly agree with available observational data, but the obvious differences, such as the spurious bumps around $M_{\text{HI}} \approx 10^{8.5}$ and $M_{\text{H}_2} \approx 10^8$ (a mass resolution limit), have been discussed in Obreschkow et al. (2009).

The predicted HI -masses remain roughly constant from $z = 0$ to $z = 2$, while H_2 -masses increase dramatically. These different evolutions are also reflected in the comoving space densities $\Omega_{\text{HI}} \equiv \rho_{\text{HI}}/\rho_c$ and $\Omega_{\text{H}_2} \equiv \rho_{\text{H}_2}/\rho_c$, where

$\rho_c(z) = 3H^2(z)/(8\pi G)$ is the critical density for closure. Here, Ω_{HI} and Ω_{H_2} only account for gas in galaxies, excluding unbound HI between the first galaxies (Becker et al. 2001) or possible H_2 in haloes (Pfenniger & Combes 1994). The simulated functions $\Omega_{\text{HI}}(z)$ and $\Omega_{\text{H}_2}(z)$ are shown in Figs. 2a, b, while Fig. 2c represents their ratio $R_{\text{mol}}^{\text{cosmic}}(z) \equiv \Omega_{\text{H}_2}(z)/\Omega_{\text{HI}}(z)$, which is closely described by the power-law

$$R_{\text{mol}}^{\text{cosmic}}(z) \approx 0.3 \cdot (1+z)^{1.6}. \quad (3)$$

The simulation yields $R_{\text{mol}}^{\text{cosmic}}(0) \approx 0.3$ and finds the crossover, $R_{\text{mol}}^{\text{cosmic}}(z) = 1$, at $z \approx 1.4$. Our model predicts that eq. (3) extends to epochs, where the first galaxies formed, but this prediction is likely to breakdown at the highest redshifts, where the formation of H_2 was inhibited by the lack of metals (Abel & Haiman 2000).

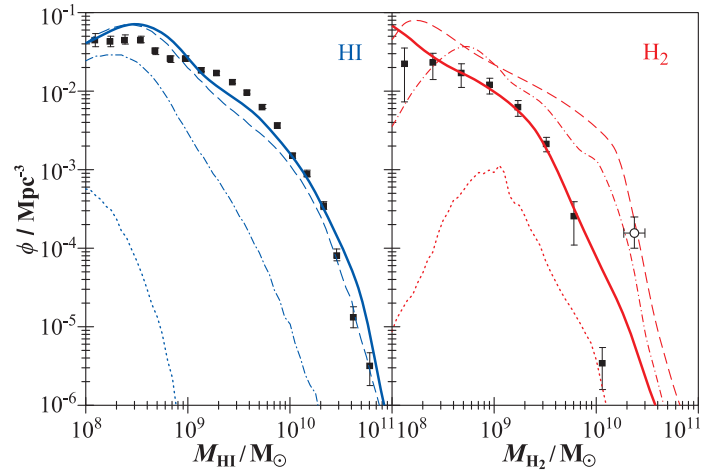


FIG. 1.— MFs of HI and H_2 . Lines show the simulation results at $z = 0$ (solid), $z = 2$ (dashed), $z = 5$ (dash-dotted), $z = 10$ (dotted). Square dots represent the empirical data and $1\text{-}\sigma$ scatter at $z = 0$ (Zwaan et al. 2005a; Obreschkow & Rawlings 2009b), and the open circle represents our density estimate at $z = 1.5$ (Section 4) based on Daddi et al. (2008).

Physically, the strong evolution of H_2/HI is essentially driven by the size-evolution of galaxies and their haloes. The Millennium Simulation assumes that the virial radius r_{vir} of a spherical halo always encloses a mass with an average density 200-times above the critical density $\rho_c \propto H^2$ (Croton et al. 2006). Hence, for a fixed halo mass, $r_{\text{vir}} \propto H^{-2/3}$. In a flat Universe this implies

$$r_{\text{vir}} \propto [\Omega_m(1+z)^3 + \Omega_\Lambda]^{-1/3}, \quad (4)$$

which asymptotically tends to $r_{\text{vir}} \propto (1+z)^{-1}$ for high z . By virtue of the theory of Fall & Efstathiou (1980), this cosmic scaling of r_{vir} results in a similar scaling of the disk radius, i.e. $r_{\text{disk}} \propto (1+z)^{-1}$, consistent with observations in the Ultra Deep Field (Bouwens et al. 2004).

For the gas-dominated galaxies in the early Universe, eq. (2) reduces to $R_{\text{mol}}^c \propto r_{\text{disk}}^{-3.2} M_{\text{g}}^{1.6}$. Yet, the cold gas masses M_{g} of individual galaxies in the simulation evolve weakly with cosmic time, due to a self-regulated equilibrium between the net inflow of gas and star formation. In fact, most of the evolution of $\Omega_{\text{HI}+\text{H}_2}$ in the redshift range $z \approx 3 - 10$ is due to the build-up of new galaxies. Therefore, $R_{\text{mol}}^c \propto r_{\text{disk}}^{-3.2} \propto (1+z)^{3.2}$. At redshifts $z \approx 1 - 10$,

¹ By contrast, a significant fraction of the stars at $z = 0$ is in massive elliptical galaxies with violent merger histories, but even those galaxies formed most stars in their spiral progenitors.

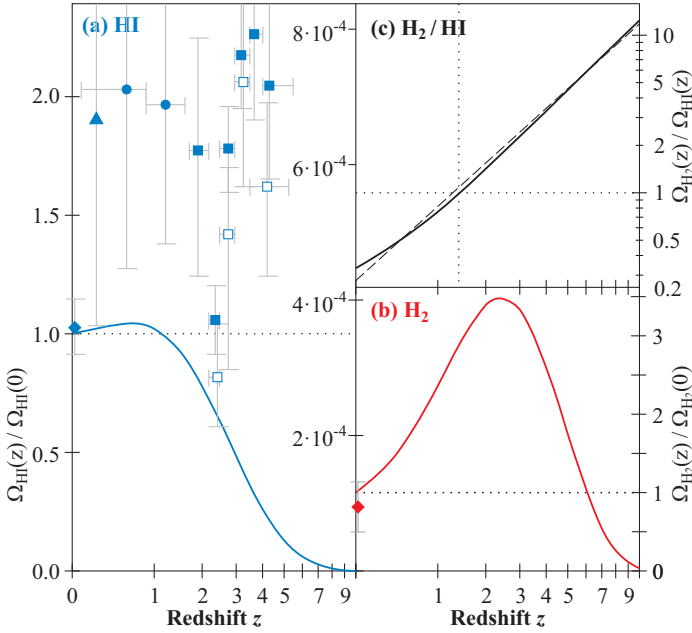


FIG. 2.— Evolution of the fractional densities of HI and H₂. Solid lines represent the simulation results and the dashed line is the power-law fit of eq. (3). The points represent observations described in Section 4.

R_{mol}^c typically takes values between 10 and 10^4 , such that eq. (1) can be approximated as $R_{\text{mol}}^{\text{galaxy}} \propto R_{\text{mol}}^c{}^{0.5}$. Hence, $R_{\text{mol}}^{\text{galaxy}} \propto (1+z)^{1.6}$, which explains the scaling of eq. (3).

The cosmic evolution of Ω_{H_2} shown in Fig. 2 can be divided in two epochs: The *early epoch* ($z \gtrsim 3$), where Ω_{H_2} increases with cosmic time, and the *late epoch* ($z \lesssim 3$), where Ω_{H_2} decreases with time. In the early epoch, $R_{\text{mol}}^{\text{galaxy}} > 1$ implies $\Omega_{\text{H}_2} \approx \Omega_{\text{HI}+\text{H}_2}$, and hence the growth of Ω_{H_2} reflects the general increase of $\Omega_{\text{HI}+\text{H}_2}$ due to the intense assembly of new galaxies. In the late epoch, $R_{\text{mol}}^{\text{galaxy}} \lesssim 1$ implies that $\Omega_{\text{H}_2} \approx R_{\text{mol}}^{\text{cosmic}} \Omega_{\text{HI}+\text{H}_2}$. At this epoch the formation of the massive galaxies in the simulation is completed, i.e. $\Omega_{\text{HI}+\text{H}_2}(z) \approx \text{const}$ and $\Omega_{\text{H}_2} \propto R_{\text{mol}}^{\text{cosmic}}$. Thus the decrease of Ω_{H_2} in this late epoch is driven by cosmic decline in $R_{\text{mol}}^{\text{cosmic}}$ or, physically, by the cosmic evolution of pressure.

3.2. Link between HI, H₂, and star formation

To discuss the global cosmic evolution of the efficiencies SFE_{HI} and SFE_{H_2} (Section 1), we shall define

$$\langle \text{SFE}_{\text{HI}} \rangle \equiv \rho_{\text{SFR}} / \rho_{\text{HI}}, \quad \langle \text{SFE}_{\text{H}_2} \rangle \equiv \rho_{\text{SFR}} / \rho_{\text{H}_2}, \quad (5)$$

where $\rho_{\text{HI}} \propto \Omega_{\text{HI}}$, $\rho_{\text{H}_2} \propto \Omega_{\text{H}_2}$, and ρ_{SFR} denote the comoving space densities of HI, H₂, and SFR.

In the semi-analytic recipes of the DeLucia-catalog, SFRs are estimated from the gas density and the dynamical time scale of the disk (Section 2.2). This Schmidt–Kennicutt law (Schmidt 1959; Kennicutt 1998) for star formation makes similar predictions to models based on cold gas pressure (e.g. Blitz & Rosolowsky 2006), and therefore the SFRs in the DeLucia-catalog are, by default, approximately consistent with our model to split cold hydrogen into HI and H₂. The evolutions of $\langle \text{SFE}_{\text{HI}} \rangle$ and $\langle \text{SFE}_{\text{H}_2} \rangle$ predicted by the simulation again reflect the marked difference between HI and H₂. They are approximated ($\sim 20\%$ relative error) by the

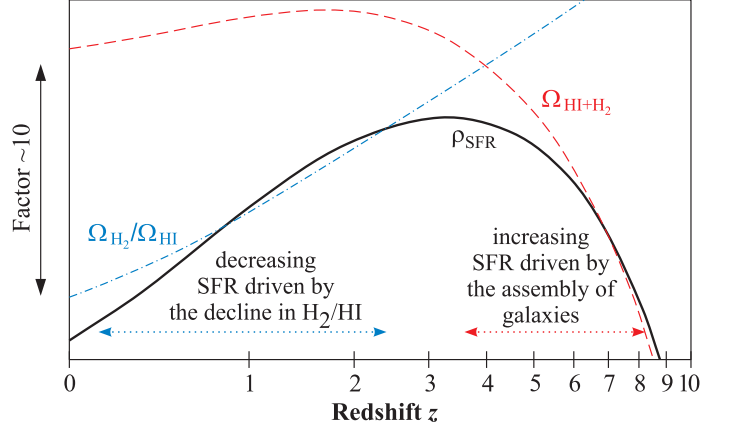


FIG. 3.— A simplistic model for the cosmic history of star formation.

power-laws,

$$\langle \text{SFE}_{\text{HI}} \rangle / [\text{Gyr}^{-1}] = 0.23 (1+z)^{2.2}, \quad (6)$$

$$\langle \text{SFE}_{\text{H}_2} \rangle / [\text{Gyr}^{-1}] = 0.75 (1+z)^{0.6}, \quad (7)$$

out to $z \approx 8$.

Due to the low power in eq. (7) $\rho_{\text{SFR}}(z)$ is approximately proportional to $\Omega_{\text{H}_2}(z)$. We can therefore apply the two cosmic epochs of $\Omega_{\text{H}_2}(z)$ introduced in Section 3.1 to the history of star formation (see Fig. 3): In the *early epoch* ($z \gtrsim 3$), ρ_{SFR} increases with cosmic time, proportionally to $\Omega_{\text{HI}+\text{H}_2}$. This increase traces the dramatic assembly of new galaxies. In the *late epoch* ($z \lesssim 3$), ρ_{SFR} decreases roughly proportionally to $\Omega_{\text{H}_2}/\Omega_{\text{HI}}$. This epoch is driven by the cosmic evolution of pressure (or density) in galactic disks. This interpretation of the history of star formation does not, in fact, conflict with the picture that star formation is ultimately defined by the accreted cold gas mass (see Section 2.2) and a Schmidt–Kennicutt law for transforming this gas into stars. Our H₂/HI-based interpretation simply adds another layer to the causal chain, by suggesting that cold gas mass and density ultimately dictate the amount of molecular material available for star formation.

The simulation also includes star formation via merger-driven starbursts, associated with the creation of the stellar spheroids of early-type spiral or elliptical galaxies. However, the cosmic star formation density caused by this process only accounts for about 1% of ρ_{SFR} , because even elliptical galaxies in the simulation formed most of their stars in their spiral progenitors.

4. COMPARISON WITH OBSERVATIONS

The DeLucia-catalog and our post-processing to assign HI and H₂, rely on established data of the local Universe. Our simulated HI- and H₂-properties at $z = 0$ are consistent with all available observations, i.e. MFs (see Fig. 1), disk sizes, and velocity profiles (Obreschkow et al. 2009). In particular, the simulated values $\Omega_{\text{HI}}(0) = 3.5 \cdot 10^{-4}$ and $\Omega_{\text{H}_2}(0) = 1.2 \cdot 10^{-4}$ are consistent with the values (diamonds in Fig. 2) derived from the MFs observed in HI- and CO-emission at $z \approx 0$ (Zwaan et al. 2005a; Obreschkow & Rawlings 2009b). At $z > 0$, the currently available data is sparse, especially in emission.

The only measurement of Ω_{HI} in emission at intermediate redshift is based on the stacking of 121 galaxies at $z = 0.24$ (Lah et al. 2007, triangle in Fig. 2). The detection is specu-

lative (see Fig. 7 in Lah et al. 2007), but roughly consistent with our simulation. All other measurements of Ω_{HI} at $z > 0$ rely on absorption detections of damped Lyman- α systems (DLAs). Respective data points from Rao et al. (2006) (circles in Fig. 2) and Prochaska et al. (2005) (filled squares) are, taken together, inconsistent with the predicted values of Ω_{HI} . By contrast, Zwaan et al. (2005b) demonstrated that the population of HI-galaxies in the local Universe can fully explain the column density distributions of DLAs out to $z = 1.5$, consistent with the nearly absent evolution of Ω_{HI} from $z = 0$ to $z = 1.5$ predicted by our simulation. At present it is therefore difficult to judge, whether the simulation is inconsistent with empirical data at these low redshifts covering 2/3 of the age of the Universe. At higher redshifts, however, the measurements of Ω_{HI} seem not conceivable with the simulated result, and even accounting for gravitational lensing by the DLAs only corrects the empirical values of Ω_{HI} by about 30% (open squares in Fig. 2, Prochaska et al. 2005). The simulated values of Ω_{HI} are likely to underestimate the real values by about a factor 2 – a plausible offset given the long list of simplifying approximations required from the N -body Millennium Simulation to our final post-processing of hydrogen in galaxies. Much progress could be expected from treating HI-masses and H₂-masses as separate quantities directly in the semi-analytic galaxy simulation. This would allow, for example, to refine the feedback-mechanisms for suppression of gas infall (explained in Croton et al. 2006), such that HI can still be accreted, while the formation of H₂ and stars is inhibited. Such a semi-analytic setting would also allow the implementation of a recipe for the large-scale dissociation of molecular gas by the radiation of newly formed stars (Allen et al. 1986). Both examples would effectively increase the amount of HI in high-redshift galaxies.

The most representative high-redshift observations of molecular gas to-date rely on two galaxies (*BzK*-4171 and *BzK*-21000) at $z \approx 1.5$, reliably detected in CO(2–1) emission by Daddi et al. (2008). Unlike other CO-sources at similar or higher z , these objects are ordinary massive galaxies with FIR-luminosities of $L_{\text{FIR}} \approx 10^{12} L_{\odot}$, selected only due to the availability of precise spectroscopic redshifts. From these two detections, we estimated the H₂-space density (empty circle in Fig. 1) as follows: The mass interval spans between the masses $M_{\text{H}_2} \approx 2 \cdot 10^{10} M_{\odot}$ and $M_{\text{H}_2} \approx 3 \cdot 10^{10}$, respectively obtained for *BzK*-4171 and *BzK*-21000 by applying the CO-to-H₂ conversion of $\alpha = 1 M_{\odot} (\text{K km s}^{-1} \text{pc}^{-2})^{-1}$ (Daddi et al. 2008). The space density of these CO-sources was approximated as the space density of FIR-sources at $L_{\text{FIR}} \approx 10^{12} L_{\odot}$, based on the fact that all (both) tar-

geted galaxies with $L_{\text{FIR}} \approx 10^{12} L_{\odot}$ revealed similar CO-luminosities L_{CO} . We estimate their space density to be $1 - 2 \cdot 10^{-4} \text{ Mpc}^{-3}$ per unit of $\log(L_{\text{FIR}})$ by extrapolating the FIR-luminosity functions (LFs) of Huynh et al. (2007). Since $L_{\text{FIR}} \propto L_{\text{CO}} \propto M_{\text{H}_2}$, we find roughly the same space density per unit $\log(M_{\text{H}_2})$. These result is consistent with the simulated H₂-MF at $z = 2$ (Fig. 1).

Considering H₂-absorption studies, Curran et al. (2004) and Noterdaeme et al. (2008) have determined H₂/HI-ratios in DLAs that showed H₂-absorption. They found H₂/HI-ratios of $\sim 10^{-6}$ to $\sim 10^{-2}$ at $z \approx 2 - 3$, clearly much smaller than our prediction for $\Omega_{\text{H}_2}/\Omega_{\text{HI}}$. We argue that measurements of H₂/HI in DLAs do not trace $\Omega_{\text{H}_2}/\Omega_{\text{HI}}$ since DLAs are by definition HI-selected objects and H₂ has a much smaller space coverage than HI. In fact, H₂-disks in galaxies are much smaller than HI-disks, especially at high z (Obreschkow & Rawlings 2009a), and even inside the H₂-disks the coverage of H₂ is small compared to HI (e.g. Ferrière 2001). A more detailed explanation of why H₂-searches in DLAs are expected to be difficult was given by Zwaan & Prochaska (2006) based on the analysis of CO-emission maps of local galaxies.

5. CONCLUSIONS

In this letter, we have predicted the cosmic evolution of HI- and H₂-masses in $\sim 3 \cdot 10^7$ simulated galaxies based on the Millennium Simulation. The predicted cosmic decline in the H₂/HI-ratio is consistent with the weak cosmic evolution of Ω_{HI} inferred from DLA-studies and recent observations revealing a significantly enhanced space density of H₂ at $z = 1.5$ (Daddi et al. 2008).

Perhaps the most important conclusion is that HI- and H₂-masses evolve very differently with cosmic time and therefore cannot be used as proportional tracers of one another, especially not for the purpose of high-redshift predictions. There is no contradiction between the large H₂-masses detected at high z , which imply values of SFE_{H_2} similar to those in the local Universe, and the weak evolution of HI, implying massively increased values of SFE_{HI} at high z .

This work is supported by the European Community Framework Programme 6, Square Kilometre Array Design Studies (SKADS), contract no 011938. The Millennium Simulation databases and the web application providing online access to them were constructed as part of the German Astrophysical Virtual Observatory. We also thank the anonymous referee for the helpful suggestions.

REFERENCES

- Abel T., Haiman Z., 2000, in *Molecular Hydrogen in Space*, Combes F., Pineau Des Forets G., eds., p. 237
 Allen R. J., Atherton P. D., Tilanus R. P. J., 1986, *Nature*, 319, 296
 Becker R. H., et al., 2001, *AJ*, 122, 2850
 Blitz L., Rosolowsky E., 2006, *ApJ*, 650, 933
 Bouwens R. J., Ilingworth G. D., Blakeslee J. P., Broadhurst T. J., Franx M., 2004, *ApJ*, 611, L1
 Croton D. J., et al., 2006, *MNRAS*, 365, 11
 Curran S. J., Murphy M. T., Pihlström Y. M., Webb J. K., Bolatto A. D., Bower G. C., 2004, *MNRAS*, 352, 563
 Daddi E., Dannerbauer H., Elbaz D., Dickinson M., Morrison G., Stern D., Ravindranath S., 2008, *ApJ*, 673, L21
 De Lucia G., Blaizot J., 2007, *MNRAS*, 375, 2
 Fall S. M., Efstathiou G., 1980, *MNRAS*, 193, 189
 Ferrière K. M., 2001, *Reviews of Modern Physics*, 73, 1031
 Gunn J. E., Gott J. R. I., 1972, *ApJ*, 176, 1
 Hopkins A. M., 2007, in *Astronomical Society of the Pacific Conference Series*, Vol. 380, *Deepest Astronomical Surveys*, Afonso J., Ferguson H. C., Mobasher B., Norris R., eds., p. 423
 Huynh M. T., Frayer D. T., Mobasher B., Dickinson M., Chary R.-R., Morrison G., 2007, *ApJ*, 667, L9
 Kennicutt R. C. J., 1998, *ApJ*, 498, 541
 Lah P., et al., 2007, *MNRAS*, 376, 1357
 Leroy A. K., Walter F., Brinks E., Bigiel F., de Blok W. J. G., Madore B., Thornley M. D., 2008, *AJ*, 136, 2782
 Noterdaeme P., Ledoux C., Petitjean P., Srianand R., 2008, *A&A*, 481, 327
 Obreschkow D., Croton D., De Lucia G., Khochfar S., Rawlings S., 2009, *ApJ*, accepted
 Obreschkow D., Rawlings S., 2009a, *ApJ*, submitted
 —, 2009b, *MNRAS*, 394, 1857

- Pfenniger D., Combes F., 1994, in Particle Astrophysics, Atomic Physics and Gravitation, Tran Thanh van J., Fontaine G., Hinds E., eds., pp. 107–113
- Pontzen A., Pettini M., 2009, MNRAS, 70
- Prochaska J. X., Herbert-Fort S., Wolfe A. M., 2005, ApJ, 635, 123
- Rao S. M., Turnshek D. A., Nestor D. B., 2006, ApJ, 636, 610
- Schmidt M., 1959, ApJ, 129, 243
- Springel V., et al., 2005, Nature, 435, 629
- Tacconi L. J., et al., 2006, ApJ, 640, 228
- Young L. M., 2002, AJ, 124, 788
- Zwaan M. A., Meyer M. J., Staveley-Smith L., Webster R. L., 2005a, MNRAS, 359, L30
- Zwaan M. A., Prochaska J. X., 2006, ApJ, 643, 675
- Zwaan M. A., van der Hulst J. M., Briggs F. H., Verheijen M. A. W., Ryan-Weber E. V., 2005b, MNRAS, 364, 1467